

Assessing the Impact of Drought on Tropical Forests



**Felipe Begliomini, Onkar Gulati, Jovana Knezevic, Yihang
She**

Advisor: Dr. C. Wheeler
A. Holcomb

AI4ER CDT
University of Cambridge

This report is submitted for
Guided Team Challenge 2023

March 2023

Table of contents

1	Introduction	1
1.1	Research Questions	2
2	Data Description and Pre-Processing	3
2.1	GEDI Data	3
2.2	Climate Variables	4
2.3	Drought Indices	5
3	Variation in Vegetation Across the Precipitation Gradient	7
4	Seasonality	10
4.1	Hypotheses to examine	10
4.2	Seasonality analysis	11
4.3	Seasonality of individual variables	11
4.4	Comparisons and correlations	12
5	Drought	15
5.1	Historic Drought	15
5.2	Recent droughts	18
5.2.1	PAI loss and recovery	19
6	Conclusion	22
References		25
Appendix A	Supplementary materials	28
A.1	Definitions	28
A.1.1	Dry seasons, dry months, dry forests	28
A.2	Seasonality	28

Chapter 1

Introduction

Onkar Gulati

Tropical forests are integral components of the global climate system, sequestering nearly 30% of annual CO₂ emissions and serving as a buffer to atmospheric heating [2]. They additionally provide habitats for a wealth of biodiversity, including a majority of terrestrial vertebrates [21]. However, these forests presently face significant anthropogenic threats including deforestation, rising temperatures, and increased wildfire risk [9].

Of particular concern is the potential impact of changing patterns in water availability, which is poorly understood. Climate change is known to be driving longer dry seasons, as well as increasingly frequent and severe droughts [12, 5]. Therefore, it is more vital than ever to evaluate the resilience of forests to such changes in their environmental water balance.

While it was previously infeasible to conduct such assessments over large scales, recent developments in remote sensing have enabled precise measurements of forest structure at high resolutions. In particular, the Global Ecosystem Dynamics Instrument (GEDI) sensor aboard the International Space Station (ISS) allows for the detection of forest structure at a higher spatial resolution and sampling density than ever before [7].

The tropical forests of South America - which account for over 40% of all remaining tropical forests - posit themselves as the ideal location in which to employ GEDI and gauge effects of changes in water availability [9]. The selection of a set of regions that display gradients in climatic and vegetation indices was conducted prior to the start of this study; these regions can be seen in Figure 1.1.

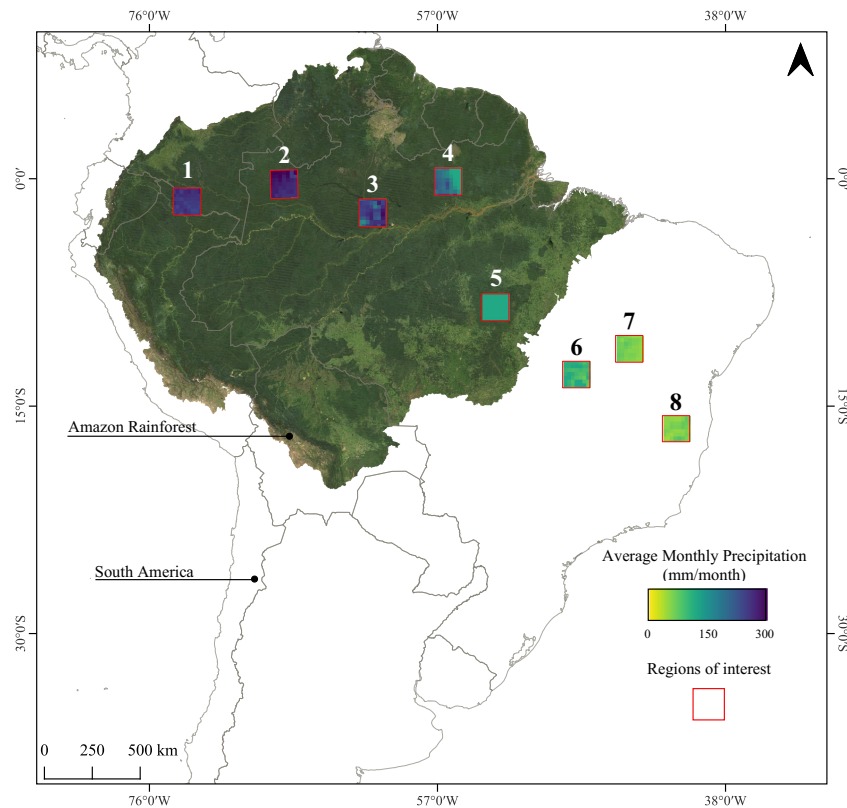


Fig. 1.1 – The eight regions of interest are quadrilaterals that exist across a climatic gradient

1.1 Research Questions

Through the use of GEDI, we specifically intend to answer the following questions:

1. To what extent is forest structure determined by the typical water availability in a given location?
2. How do forests across the climatic spectrum react to seasonal variations in precipitation, temperature, and radiation?
3. How does anomalous drought affect forest structure over short and long periods of time?

Chapter 2

Data Description and Pre-Processing

Felipe Begliomini

2.1 GEDI Data

GEDI is the first spaceborne LiDAR system designed for pantropical ecosystems applications [8]. The sensor has been sampling full-waveform LiDAR data (1064 nm) from 51.6° to -51.6° latitude since 2019. GEDI footprints have a nominal spatial resolution of 25 m in diameter, acquired every 60 m, in eight parallel transects separated 600 m from each other. The data is available in different processing levels, ranging from geolocated LiDAR raw waveforms to derived bio-physical parameters [13]. For our analysis, we used GEDI Level 2B (L2B) acquired from UMD's website (<https://gedi.umd.edu>), and extracted bio-physical variables to investigate the effects of droughts on vegetation: the Plant Area Index (PAI) as well as vertical distribution of PAI sliced in 5 m intervals. PAI is defined as the total area of canopy structure elements (e.g., leaves, branches, trunk) per unit ground surface and is widely used as a proxy to characterize the canopy structure [28].

The temporal extent of our dataset comprised samples acquired from April 2019 to May 2022. Since GEDI data was downloaded as worldwide granules, we first did a spatial query to select only the shots within the eight regions defined as our study area. Table 2.1 describes the filters applied after the spatial reduction to identify bad-quality shots, as GEDI's user guide and previous studies recommended [22]. Finally, a land cover map [25] was used to filter only the shots that landed in the studied biomes. We extracted a 3x3 window centered at the GEDI shot location, and only the samples where all pixels were classified as savanna

Table 2.1 – Parameters and criteria used to filter the GEDI dataset

Parameter	Criteria
Quality Flag	= 1
PAI	> 0
Sensitivity	≥ 0.95
Beam mode	= Full power

or forest were incorporated in the final dataset. After all filtering steps, 8,239,373 shots were selected to perform the subsequent analysis.

2.2 Climate Variables

We selected a range of climate variables and compared them with GEDI data metrics to infer if seasonal patterns' anomalies could drive changes in the vegetation structure. The datasets were derived from global remote sensing and had an extensive long-term archive (>20 years). They were available in Google Earth Engine (GEE), which was also used to perform the imagery pre-processing. We selected two decades of data (from 2001 to 2022) to extract long-term seasonality patterns for the studied regions. Quality control was performed using the available native quality bands, and masks were applied image-by-image to remove bad-quality pixels. Considering the different temporal resolutions, all datasets were aggregated monthly to allow consistency in the analysis. The following datasets were selected to extract the studied climate variables:

1. CHIRPS: The Climate Hazards Group InfraRed Precipitation (CHIRPS) provided the daily precipitation data (mm/day), converted to cumulative monthly precipitation. The dataset is derived from the combination of satellite data and a network of weather stations at a spatial resolution of 0.05° [10].
2. MODIS: The Moderate Resolution Imaging Spectroradiometer (MODIS) provided surface temperature, the absorbed Fraction of Photosynthetically Active Radiation (FPAR), and Potential Evapotranspiration (PET). Detailed information about MODIS parameters is given in Table 2.2. We aggregated PET to cumulative monthly data, while FPAR and surface temperature were reduced to monthly averages.
3. ERA5: The European Centre for Medium-Range Weather Forecasts Reanalysis v5 (ERA5) provided the average monthly surface net solar radiation data (J/m^2). The product is the difference between the total solar downward radiation (direct and diffuse) and the reflected solar radiation. The data is available at a spatial resolution of 0.1° .

Table 2.2 – MODIS variables description

Parameter	Description	Product	Temporal Resolution	Spatial Resolution
Temperature	Land Surface Temperature (<i>Kelvin</i>)	MOD11A1	Daily	
FPAR	Amount of radiation within the photosynthetically active spectral range (400-700 nm) absorbed by green vegetation (%)	MOD15A2H	8-day composite	500
PET	Evapotranspiration rate if water availability is not limited ($kg/m^2/8day$)	MOD16A2		

2.3 Drought Indices

Alterations in the precipitation patterns are responsible for causing dry spells [16]. However, quantifying critical characteristics of drought events (e.g., intensity, duration, spatial extent) from climate variables alone is challenging. Therefore, drought indices were developed to combine environmental data and leverage monitoring [19]. Palmer Drought Severity Index (PDSI) and the Standardized Precipitation Evapotranspiration Index (SPEI) are widely used as proxies for identifying drought events [32]. PDSI is calculated from precipitation, moisture supply, runoff, and evaporation demand data [31], while SPEI is based on the climatic water balance (PET – precipitation) [29]. Both indices are calibrated at a regional scale, considering long-term climate data to create a baseline used to calculate the index output. The main difference between them lies on the temporal flexibility for retrieving the indices. While PSDI can only be calculated for a fixed time range, SPEI can be computed with a wider retroactive time span (1-48 months).

We extracted PDSI from GEE at the TerraClimate dataset, at a resolution of approximately 4000 m in monthly composites. Since no SPEI dataset is provided by GEE for the studied area, we generated the index from precipitation (CHIRPS) and PET (MODIS) data. We calculated the monthly climatic water balance for the 22-years' time series and used a python library (<https://pypi.org/project/spei/>) to calculate SPEI (1, 3, 6, 9, 12 and 18 months) for each region of interest. Finally, we classified PSDI and SPEI values into climatic events classes (Table 2.3) [20].

Table 2.3 – Climatic event classification based on drought indices

Class	SPEI value	PSDI value
Extremely wet	Greater than 2.00	Greater than 4.00
Severely wet	1.50 to 1.99	3.00 to 3.99
Moderately wet	1.00 to 1.49	2.00 to 2.99
Slightly wet	0.50 to 0.99	1.00 to 1.99
Near normal	-0.49 to 0.49	-0.99 to 0.99
Mild dry	-0.99 to -0.50	-1.99 to -1.00
Moderately dry	-1.49 to -1.00	-2.99 to -2.00
Severely dry	-1.99 to -1.50	-3.99 to -3.00
Extremely dry	Less than -2.00	Less than -4.00

Chapter 3

Variation in Vegetation Across the Precipitation Gradient

Jovana Knezevic

In our initial investigation, we examined the following questions: do vegetation characteristics vary across regions that experience different precipitation patterns? Can moist forests maintain dense canopies with less annual rainfall? Can we observe vegetation adaptations that allow forests to cope with water deficits?

We analyzed aggregate climate and vegetation data across eight South American regions that are positioned along the latitudinal climatic gradient (Figure 1.1). The regions are classified into two different biomes: regions 1-5 represent the Amazon moist tropical forest, while regions 6-8 are designated as Seasonally Dry Tropical Forests (SDTFs).

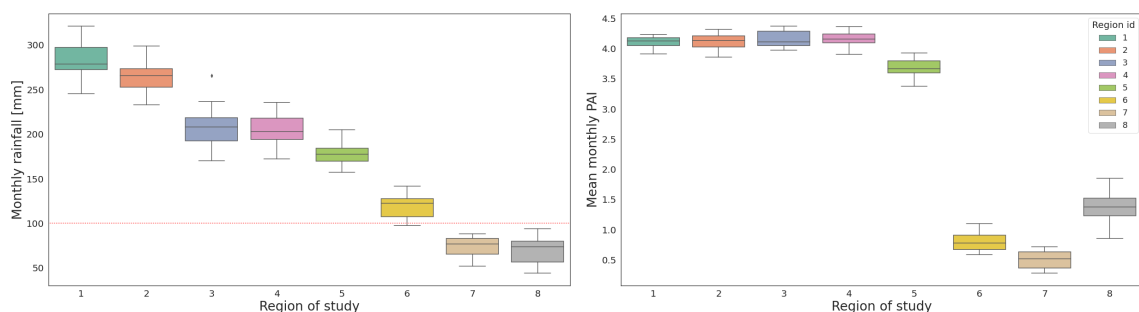


Fig. 3.1 – Average monthly rainfall versus PAI for each region. a) Mean monthly rainfall with red dotted line representing the 100mm threshold for a “dry month”. b) Mean monthly PAI. Regions 1 through 4 maintain a comparable vegetation index despite variations in precipitation.

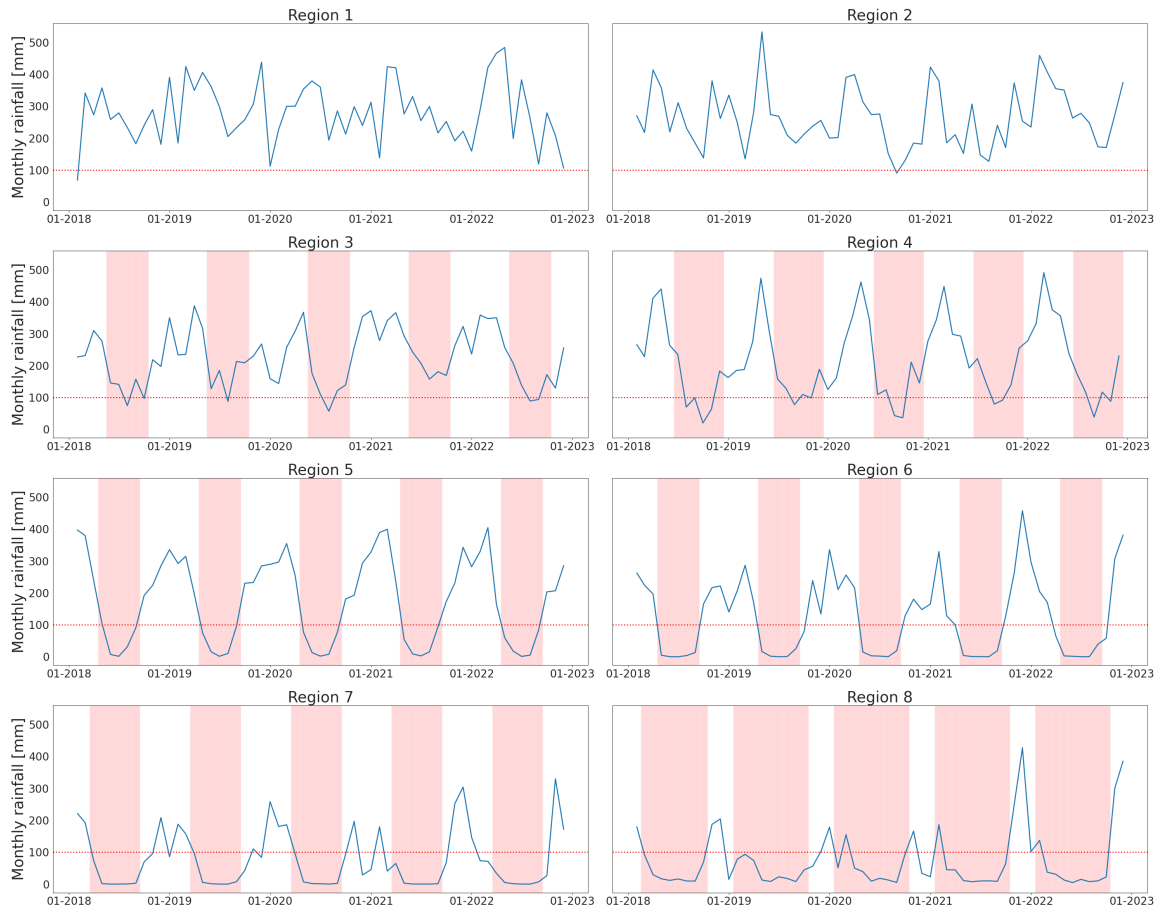


Fig. 3.2 – Precipitation variations across regions. Red shading indicates the average dry season. Regions with minimum monthly precipitation above 150 mm, such as regions 1 and 2, are labeled as having no dry season (A.1.1). Regions 5, 6, 7, and 8 experience consecutive months with less than 100 mm of rain.

Figure 3.1 a) and Figure 3.2 show variations across regions in the amount and the distribution of rainfall throughout the year. Regions 1, 2, 3, and 4 vary in mean rainfall and occurrence of dry seasons, but receive consistently high precipitation, while dry months dominate in regions 6, 7 and 8 [26]. Region 5 combines the characteristics of both biomes, with substantial rainfall during its wet season, and consecutive dry months during the dry season. Figure 3.1 b) shows that despite variations in rainfall, regions 1 through 4 maintain high and comparable PAI values, with region 5 being the only moist tropical forest region where we observe a decrease in average PAI. In contrast, STDF regions have a significantly lower PAI and significantly higher PAI coefficient of variation than the Amazon regions, indicating the presence of significant leaf abscission and regrowth during the year. This observation is consistent with shorter canopies and deciduousness, the primary adaptation mechanisms of SDTFs to dry conditions [1].

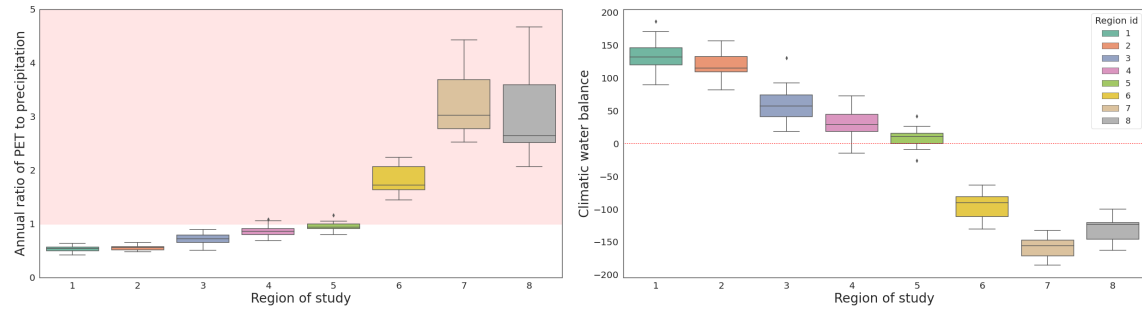


Fig. 3.3 – Two measures of water balance. Both measures indicate that regions 6, 7, and 8 are in a state of water deficit, while region 5 is just above the threshold. a) The ratio of total annual PET to precipitation. A red highlighted region indicates a PET to precipitation ratio greater than 1, which signifies the transition to SDTFs [1]. b) The annual climatic water balance. Negative values indicate a water deficit, where water needs of vegetation surpass available rainfall [14].

Observations of regions 1-4 indicate that moist forests have the ability to maintain a consistent vegetation cover within a range of precipitation patterns. However, lower PAI is seen in region 5, which is the Amazon region with most water deficit (Figure 3.1). The ecosystem transitions to seasonally dry tropical forests in regions 6, 7, and 8 as we move further into the zone of water deficit. We hypothesize that as forest's water balance crosses the water deficit line, decrease in vegetation cover follows. As the climatic profile shifts to one dominated by water deficit, forests with lower PAIs, shorter canopies and dry-season adaptations become prevalent.

Chapter 4

Seasonality

Yihang She

To better understand typical responses of vegetation to drought, we run seasonality analysis to extract seasonal components from time sequence data of PAI and various climate variables. In the following sections, we will introduce the hypothesis we want to examine, the method we will use, and insights revealed by the seasonal components.

4.1 Hypotheses to examine

How vegetation across different regions respond to climate variables: As aforementioned, geographic conditions vary significantly across our selected regions. The Amazon mainly consists of moist forests with no significant dry months, while SDTFs have greater climatic variability [11, 17]. Thus it is not surprising that the dynamics of drought will have significant variations across the whole study area. However, responses of moist forests in the Amazon are less well studied compared to the SDTFs. With the extracted seasonal components of PAI and climate variables for both regions, we hope to conduct a fine-grained analysis of the response of vegetation to dry conditions.

Green-up or not: what GEDI can tell: "Green-up" refers to the increase of spectral reflectance of the forest canopy in a typical dry season [3]. So far, whether or not Amazonian forests experience "green-up" is still debatable [3, 18, 23, 27]. The "green-up" based on vegetation indices from optical satellites (e.g. MODIS) is often questioned by the coarse resolution and atmospheric artifacts of the data [3, 27]. For instance, [18] data from both MODIS and GLAS, which is a LiDAR sensor, finds no evidence of significant "green-up" in

the southern Amazon forest. Thus we wish to investigate if GEDI, as the latest generation of LiDAR, can provide any new insights.

4.2 Seasonality analysis

Decomposition of a time sequence: Time sequence decomposition allows us to understand the underlying patterns of the data. Each data point D_t at time step t is decomposed into three components, namely trend T_t , seasonality S_t , and residual R_t :

$$D_t = T_t + S_t + R_t \quad (4.1)$$

Where T_t represents the long-term trend; S_t represents the periodic pattern; and R_t represents the remaining variability of the data. We are especially interested in the seasonality component as it reveals patterns of the time sequence over a certain period.

Implementation details: We apply the Seasonal-Trend decomposition using Loess (STL) [6] for our seasonality analysis. Compared to a simple moving average, STL interpolates the time sequence to mitigate the impacts of outliers.

We run STL for monthly data of both PAI and a wide range of climate variables. The time sequence of climate variables covers a long time period from 2001 until 2022. Compared to climate variables, the PAI from GEDI is only available from 2019 to 2022 and for some months the data is missing. For such reasons, region 3 is not considered for the seasonality analysis as it has significant data gaps even after interpolation (see Figure A.1).

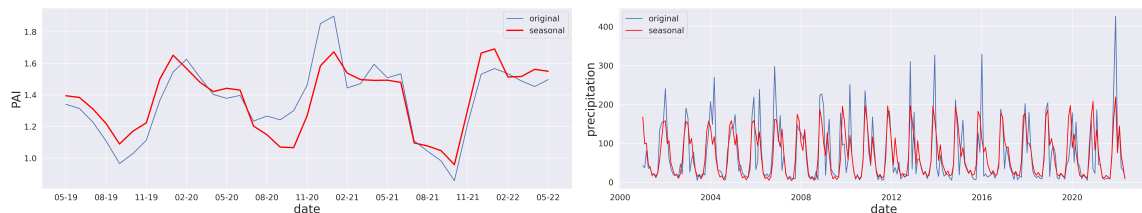


Fig. 4.1 – Seasonal component vs. original data. We add the mean of the original data to the seasonal component for a better comparison. Variables for both vegetation and climate show clearly annual patterns.

4.3 Seasonality of individual variables

Vegetation contrasts: As can be seen in Figure 4.2, both the PAI and the FPAR are higher on average and less variable in the Amazon compared to those in the SDTFs, indicating that

the Amazon possesses more dense forests with more active photosynthesis in general. This is aligned with the fact that the Amazon is dominated by tropical moist forests which are known to be more productive than the SDTFs. Indeed, forests in these two regions display different responses to climate variables, which we will discuss in Section 4.4.

Climate contrasts: It can be seen in Figure 4.2 that polygons located in the Amazon receive significantly more precipitation and are usually water-sufficient. Also, temperatures there are lower on average and show fewer variations compared to the SDTFs. While this indicates that the Amazon is adapted to a more moist and more stable climatic environment, some difference among polygons in the region is non-negligible: region 5 experiences both high and low rainfalls in extremes (Figure A.6), which is probably due to its location at the transition zone between the Amazon and the SDTFs. Interestingly, we also observe a typical "green-up" in region 5, which we will detail in Section 4.4.



Fig. 4.2 – Seasonality of vegetation and climate variables in region 1 vs. in region 8. Region 1 and 8 is located in the Amazon and the SDTFs, respectively. The seasonality of each variable from region 1 clearly contrasts its counterpart in region 8, in terms of both vegetation and climate.

4.4 Comparisons and correlations

We compared the seasonality between PAI and various climate variables (Table A.1). We found that the response of vegetation seasonality to precipitation has displayed distinct patterns across different regions.

Influence of precipitation across regions: similarities and differences: For both the Amazon and the SDTFs, we observe that precipitation has a boosting effect on vegetation growth after one or two months (Figure 4.3). However, this boosting effect comes faster and stronger in the regions of the SDTFs compared to those in the Amazon (Table 4.1). Thus

precipitation seems to play a more dominant role in the growth of vegetation in the SDTFs, where the climate is dryer and more variable.

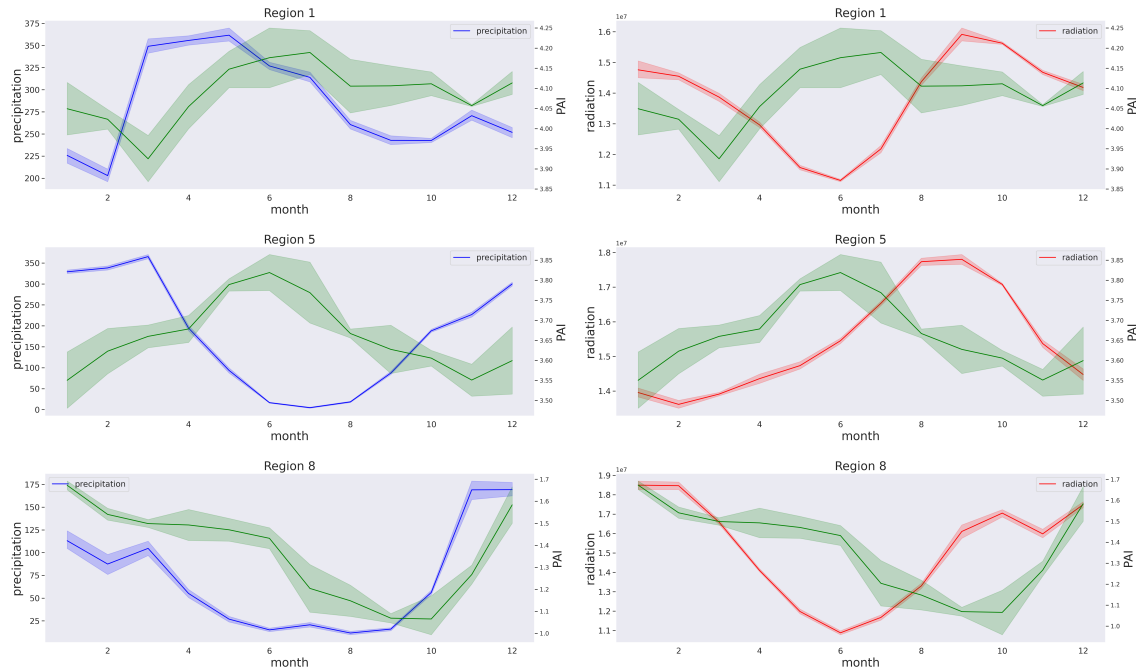


Fig. 4.3 – Comparison of the seasonality between PAI and the climate variables precipitation and radiation. Region 1, 5, 8 is located at the Amazon, the transition zone and the SDTFs, respectively. Region 5 displays a typical "green-up".

Typical green-up observed in the transition zone: Besides precipitation, would any other factors be a driving factor of vegetation growth? Interestingly, we observe a very typical green-up phenomenon driven by radiation in the dry season in region 5. A dry season usually starts with decreasing precipitation and increasing radiation. Despite less precipitation, vegetation there keeps growing with the increasing radiation. As can be seen in Figure 1.1, region 5 is located at the transition zone between the Amazon and the SDTFs, and the seasonality of individual variables suggests that it is dominated by moist tropical forests and meanwhile experiences more variable climate (Appendix A.2). Therefore, though region 5 regularly experiences dry seasons as the other regions in the SDTFs, we speculate that the water content in the soil is still sufficient to allow vegetation growth driven by increasing radiation, thanks to the heavy rainfall in the region before the dry season.

Table 4.1 – Correlation coefficients between the seasonal PAI and precipitation. We correlates the seasonality of PAI with precipitations that occurred at the same month ($precipitation_0$), 1-month ago ($precipitation_1$) and 2-month ago ($precipitation_2$) to better understand the influence of precipitation. As can be seen, the PAI in regions 6, 7, and 8 at the SDTFs display strongly positive correlations with the precipitation occurring 1 month ago. In contrast, the correlations between PAI and precipitation in regions 1 and 2 at the Amazon are not as strong as those in the SDTFs.

Region	1	2	4	5	6	7	8
$precipitation_0$	-0.018	0.368	-0.507	-0.613	0.837	0.860	0.373
$precipitation_1$	0.537	0.556	-0.086	-0.261	0.865	0.917	0.770
$precipitation_2$	0.598	0.500	0.338	0.249	0.613	0.699	0.756

Chapter 5

Drought

Onkar Gulati

In the assessment of precipitation anomalies, the constraints on GEDI availability and the relative infrequency of droughts make it difficult to observe the same region under differing levels of abnormal water deficit. To overcome this, we employ *space-for-time-substitution*, a technique commonly used to assess impacts of otherwise unobservable long-term ecological processes, in which temporal variation is replaced with spatial variation [30]. In this context, we are able to infer how varying degrees of anomalous water deficit impact forests by comparing forest structure (as measured by PAI) across regions which span a spectrum of historic water balance conditions.

While drought is broadly indicated as ‘a deficit of water relative to normal conditions,’ it is considered impractical to encapsulate this within a single mathematical definition [15]. We utilise two prominent drought indices, PDSI and SPEI, to quantify historic and short-term drought respectively across our regions of interest.

5.1 Historic Drought

The Palmer Drought Severity Index (PDSI) computes the severity of drought in a given region through use of a supply-and-demand model of soil moisture, with supply corresponding to precipitation and demand to evapotranspiration, along with underlying soil conditions as additional inputs (see Ch. 2). PDSI is noted to capture long-term drought exceptionally well, although its utility on timeframes shorter than a year is highly contested.

Recent field measurements have indicated short-term (mean 5 years) vegetation-type conversion following drought-induced tree mortality [4]. In light of these results, we first observed any potential correlations of PAI against mean 5-year PDSI for 128 subregions within our regions of interest (with each quadrilateral divided into a 4x4 grid).

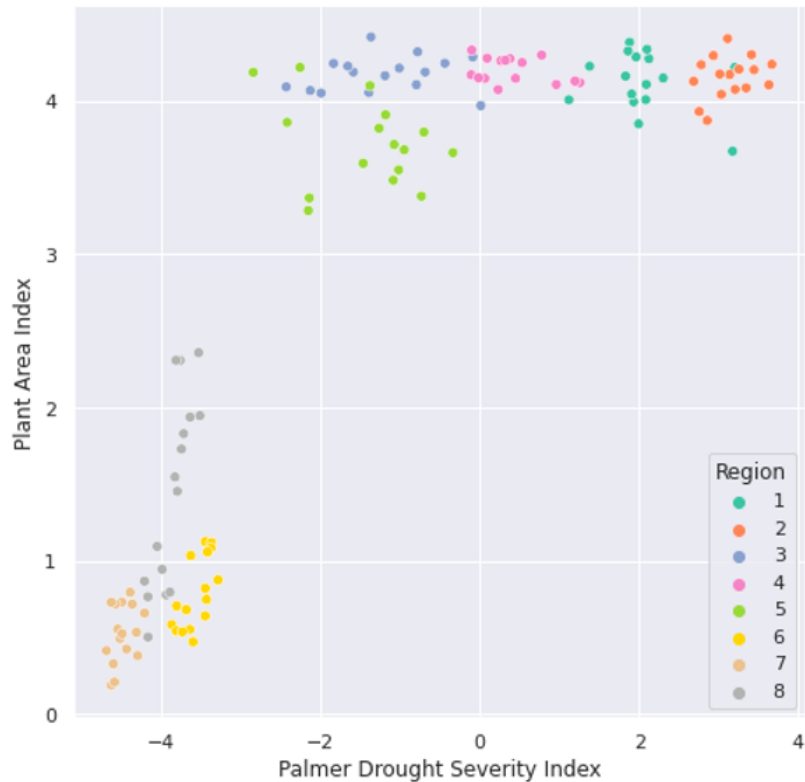


Fig. 5.1 – Mean Plant Area Index (2019 - 2022) as observed by GEDI increases sharply with Mean Palmer Drought Severity Index (2014 – 2019) for Cerrado regions, but appears insensitive to water balance changes in the Amazon regions

Two clear clusters emerge here: one consisting of regions within SDTFs (regions 6-8) and one consisting of those within the Amazon (regions 1-5). The former presents a marked uptick in present PAI for subregions which have experienced lower levels of 5-year drought, while the latter exhibits relatively little variation in PAI.

Running linear regressions within these two clusters confirms that while the correlation is statistically significant in both cases ($p < 0.001$), the dependence is stronger for the first ($R^2 = 0.247$) as opposed to the second ($R^2 = 0.096$). These regressions do assume that the true relationship here is that of parametric linear functions and not, for example, a sigmoid function. Analysis of further regions, particularly those that have a PAI within the range of 2-3, would be required to confirm the nature of this relationship.

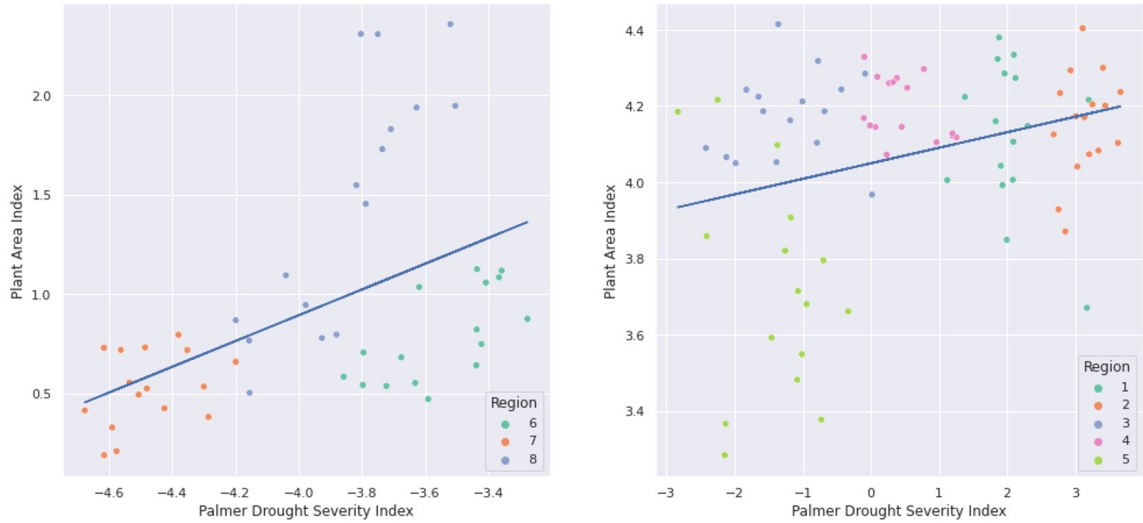


Fig. 5.2 – Regression of Mean Plant Area Index (2019 - 2022) as observed by GEDI against Mean Palmer Drought Severity Index (2014 – 2019) for regions in SDTFs (left) and Amazon (right)

These observations lead to a similar conclusion to that obtained from our seasonality analysis: forest structure depends heavily on water balance only while there is a water deficit.

In an attempt to test for persistent effects of drought, we then iteratively alter the start date of the interval that PDSI was averaged over, with a maximum interval of 20 years (1999 - 2019). Regressions against each of these variables result in statistically significant correlations, but with varying coefficients of determination.

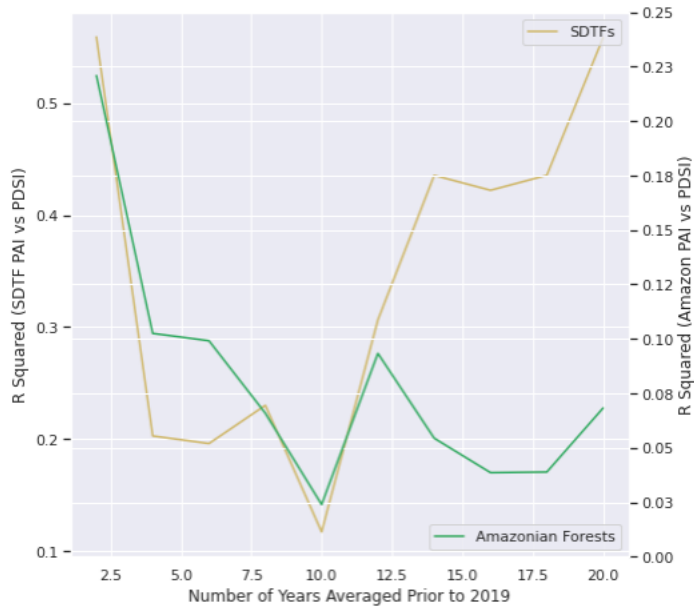


Fig. 5.3 – Coefficients of determination for regressions of PAI against PDSI averaged over a variable time period ending in 2019 for SDTFs (yellow, left axis) and Amazon (green, right axis)

While both SDTFs and Amazonian forests show strong relationships with recent PDSI (2 year interval), they diverge notably with long-term PDSI, with the correlation of STDF PAI with PDSI increasing notably for longer intervals of PDSI. This perhaps indicates that, in SDTFs, persistent drought can result in adaptation towards lower biomass and therefore lower PAI. It could also point towards the resilience of Amazonian forests, where the correlation is not seen to increase notably beyond the 10 year mark.

5.2 Recent droughts

Jovana Knezevic

The ideal study of forest response to drought would include observations of vegetation structure before, during and after a drought. With only three years of GEDI data available, we looked for evidence of drought events in our study regions in the period of 2019 to 2022. We focused our study on the moist tropical regions of Amazon (regions 1-5).

To detect anomalous dry periods, we derived mean monthly SPEI index for each Amazon region. We found that during the 2019-2022 period, only the region 2 experienced an extreme drought ($SPEI < -2$), as evidenced by SPEI-3 values in Figure 5.4. Specifically, region 2 experienced two consecutive droughts, one at the end of 2020, and one in the middle of 2021,

with both SPEI-3 and SPEI-12 values reaching extreme drought levels (Figure 5.5).

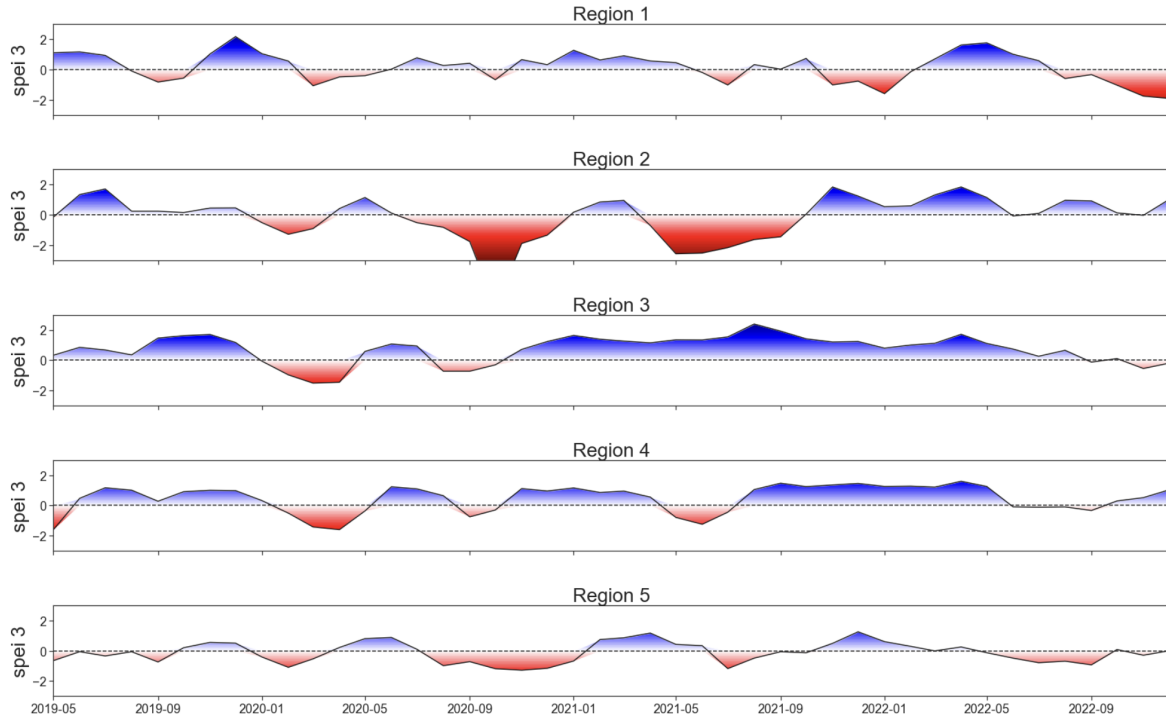


Fig. 5.4 – 3-month SPEI for each Amazon region. Only region 2 experienced a significant drought ($\text{SPEI } 3 < -2$) during the period of GEDI data collection.

5.2.1 PAI loss and recovery

By examining the monthly time series of total PAI in Figure 5.5, we discovered a significant loss of vegetation and subsequent recovery that coincide with the extreme drought event of 2020, with the mean PAI value decreasing from 4.31 in May, to 3.86 in November of 2020. Then, with the increase of precipitation in 2021, we see a quick partial recovery within 3 months. A longer drought of slightly milder intensity follows, and the region experiences a more gradual loss of PAI that continues even after the drought ends.

Additionally, we took advantage of GEDI's ability to provide vertical PAI vegetation profile and investigated how drought-induced PAI losses vary with vegetation height. Figure 5.6 shows that the upper canopy (height $> 15\text{m}$) underwent the most significant PAI loss during the 2020 drought.

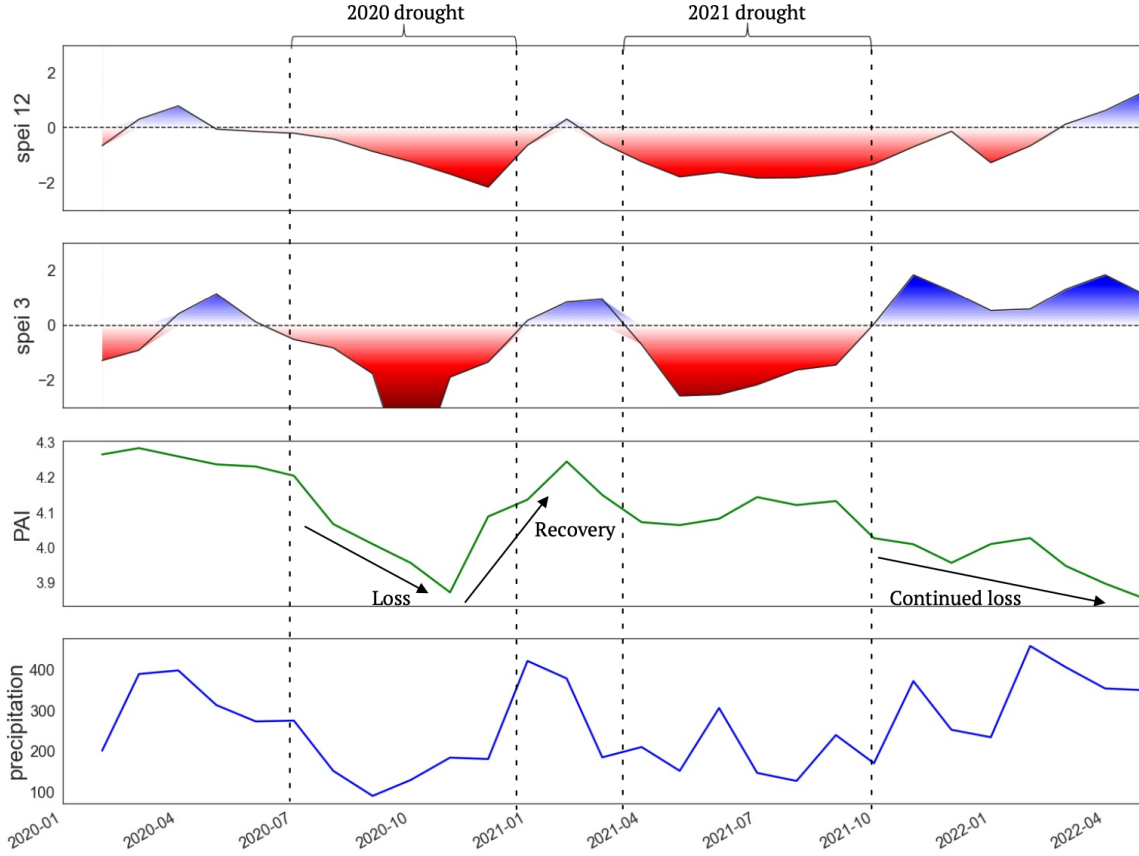


Fig. 5.5 – Drought related PAI loss and recovery.

Our findings suggest that moist forests are sensitive to extreme drought events, and the level of sensitivity (expressed as PAI loss) varies with intensity and length of the event. The undercanopy appears more resistant to short-term drought, and the primary loss of vegetation cover happens in the upper canopy. These results confirm the field findings in [24] that tall upper canopy trees experience more pronounced drought effects. The region exhibited some resiliency by managing to recover to partial pre-drought PAI levels after the first drought, but we see a continued decline in PAI levels after the second drought. We speculate that forest's recovery capacity may be diminished following multiple consecutive droughts. We suggest further monitoring of this region's recovery as more recent GEDI data becomes available.

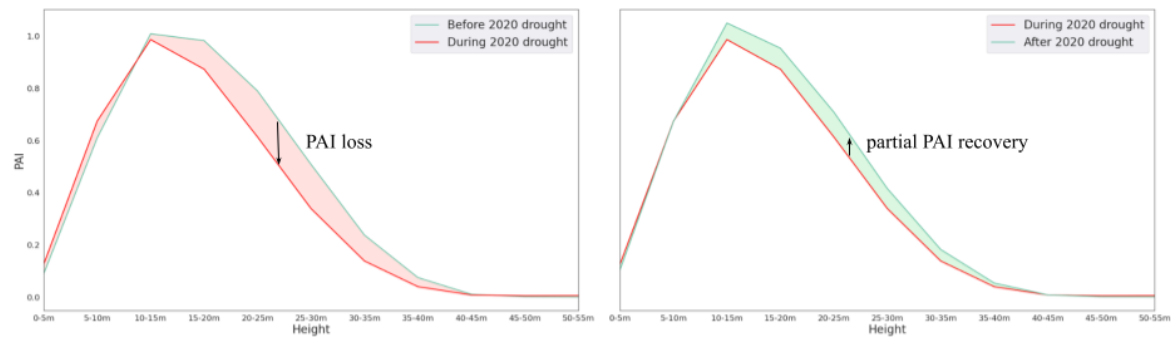


Fig. 5.6 – PAI loss and recovery depending on forest height. Primary PAI loss happens in the canopy (height > 15m), with understory being largely unaffected.

Chapter 6

Conclusion

Felipe Begliomini

Through evaluating correlations between a host of climate metrics and GEDI-derived proxies of forest structure, we arrived at the following conclusions:

1. To what extent is forest structure determined by the typical water availability in a given location?

Our analyses suggest that the Amazon is resilient to considerable variations in precipitation, being able to maintain comparable PAI values even when comparatively low quantities of water are available. However, when forest regions fall into a water deficit, reductions on PAI and adaptive forest responses to dryness are observed. We suggest future studies focus on monitoring Region 5, as it is the evaluated Amazonian region closest to being in a water deficit. In the context of climate change and increasing dry seasons, it is important to constantly monitor the driest areas of moist tropical forest. Once those forests are not adapted to long periods of shortage in rainfall, further reductions on precipitation makes them more susceptible to transitioning to SDTFs.

2. How do forests across the climatic spectrum react to seasonal variations in precipitation, temperature, and radiation?

The seasonality analysis clearly highlights the vegetation and climate difference in the Amazon and the STDFs. All variables displayed annual seasonality. The seasonal PAI displays different patterns of response to precipitation depending on the regions.

Precipitation has boosting effects to vegetation in both the Amazon and the STDFs, even though the last seems more sensitive to water availability. Additionally, with GEDI data we observe a typical "green-up" phenomenon in the transition zone between the Amazon and the STDFs, which provides new insights to the on-going debate regarding the "green-up" in the region of interest. However, it is important to note that the "green-up" effect was observed in the long-term analysis trend, which means that it might be related to normal variations on precipitation patterns (e.g., normal dry and wet seasons). The analyses provided in Chapter 5 shown that when vegetation experienced drought seasons outside the normal range, negative effects in forest structure metrics are observed.

3. How does anomalous drought affect forest structure over short and long periods of time?

Historic drought is found to affect PAI significantly in climates that are under regular water stress, but less significantly so in climates where water is readily available. Persistent drought (indicative of drought metrics averaged over more than 10 years) correlates with present PAI only for SDTFs and not Amazonian forests, indicating long-term adaptation in SDTFs, resilience in Amazonian forests, or both. Short-term droughts do cause clear changes in PAI, particularly in the upper canopy.

Access to the Code: All codes used to generate the results in this study are available at a GitHub repository via the following link: <https://github.com/4C-Guided-Team-Challenge/drought-with-gedi/releases/tag/v0.1.0>.

Acknowledgements

We would like to extend our gratitude to the supporters of this project. In particular, we thank our advisors Amelia Holcomb and Dr. Charlotte Wheeler for their extensive guidance throughout the course of the project. We're also extremely thankful to Dr. Michael Dales (*Department of Computer Science Technology*) for helping us access Sherwood, without which this project would not have been possible. Finally, we appreciate the ongoing support of everyone at the Cambridge Center for Carbon Credits.

References

- [1] Allen, K., Dupuy, J. M., Gei, M. G., Hulshof, C., Medvigy, D., Pizano, C., Salgado-Negret, B., Smith, C. M., Trierweiler, A., Bloem, S. J. V., Waring, B. G., Xu, X., and Powers, J. S. (2017). Will seasonally dry tropical forests be sensitive or resistant to future changes in rainfall regimes? *Environmental Research Letters*, 12:023001.
- [2] Artaxo, P., Hansson, H. C., Machado, L. A. T., and Rizzo, L. V. (2022). Tropical forests are crucial in regulating the climate on earth. *PLOS Climate*, 1(8):e0000054.
- [3] Asner, G. P. and Alencar, A. (2010). Drought impacts on the amazon forest: the remote sensing perspective. *New phytologist*, 187(3):569–578.
- [4] Batllori, E., Lloret, F., Aakala, T., Anderegg, W. R., Aynekulu, E., Bendixsen, D. P., Bentouati, A., Bigler, C., Burk, C. J., Camarero, J. J., et al. (2020). Forest and woodland replacement patterns following drought-related mortality. *Proceedings of the National Academy of Sciences*, 117(47):29720–29729.
- [5] Chiang, F., Mazdiyasni, O., and AghaKouchak, A. (2021). Evidence of anthropogenic impacts on global drought frequency, duration, and intensity. *Nature communications*, 12(1):2754.
- [6] Cleveland, R. B., Cleveland, W. S., McRae, J. E., and Terpenning, I. (1990). Stl: A seasonal-trend decomposition. *J. Off. Stat.*, 6(1):3–73.
- [7] Dubayah, R., Armston, J., Healey, S. P., Bruening, J. M., Patterson, P. L., Kellner, J. R., Duncanson, L., Saarela, S., Ståhl, G., Yang, Z., et al. (2022). Gedi launches a new era of biomass inference from space. *Environmental Research Letters*, 17(9):095001.
- [8] Dubayah, R., Blair, J. B., Goetz, S., Fatoyinbo, L., Hansen, M., Healey, S., Hofton, M., Hurt, G., Kellner, J., Luthcke, S., et al. (2020). The global ecosystem dynamics investigation: High-resolution laser ranging of the earth’s forests and topography. *Science of remote sensing*, 1:100002.
- [9] Feng, X., Merow, C., Liu, Z., Park, D. S., Roehrdanz, P. R., Maitner, B., Newman, E. A., Boyle, B. L., Lien, A., Burger, J. R., et al. (2021). How deregulation, drought and increasing fire impact amazonian biodiversity. *Nature*, 597(7877):516–521.
- [10] Funk, C., Peterson, P., Landsfeld, M., Pedreros, D., Verdin, J., Shukla, S., Husak, G., Rowland, J., Harrison, L., Hoell, A., et al. (2015). The climate hazards infrared precipitation with stations—a new environmental record for monitoring extremes. *Scientific data*, 2(1):1–21.

- [11] Gatti, L. V., Basso, L. S., Miller, J. B., Gloor, M., Gatti Domingues, L., Cassol, H. L., Tejada, G., Aragão, L. E., Nobre, C., Peters, W., et al. (2021). Amazonia as a carbon source linked to deforestation and climate change. *Nature*, 595(7867):388–393.
- [12] Guo, J., Hu, S., and Guan, Y. (2022). Regime shifts of the wet and dry seasons in the tropics under global warming. *Environmental Research Letters*, 17(10):104028.
- [13] Kellner, J. R., Armston, J., and Duncanson, L. (2021). Algorithm theoretical basis document for gedi footprint aboveground biomass density. *Earth and Space Science*, page e2022EA002516.
- [14] Khoury, S. and Coomes, D. A. (2020). Resilience of Spanish forests to recent droughts and climate change. *Global Change Biology*, 26(12):7079–7098.
- [15] Lloyd-Hughes, B. (2014). The impracticality of a universal drought definition. *Theoretical and Applied Climatology*, 117:607–611.
- [16] Marengo, J. A. and Espinoza, J. C. (2016). Extreme seasonal droughts and floods in amazonia: causes, trends and impacts. *International Journal of Climatology*, 36(3):1033–1050.
- [17] Marengo, J. A., Souza Jr, C. M., Thonicke, K., Burton, C., Halladay, K., Betts, R. A., Alves, L. M., and Soares, W. R. (2018). Changes in climate and land use over the amazon region: current and future variability and trends. *Frontiers in Earth Science*, 6:228.
- [18] Morton, D. C., Nagol, J., Carabajal, C. C., Rosette, J., Palace, M., Cook, B. D., Vermote, E. F., Harding, D. J., and North, P. R. (2014). Amazon forests maintain consistent canopy structure and greenness during the dry season. *Nature*, 506(7487):221–224.
- [19] Mukherjee, S., Mishra, A., and Trenberth, K. E. (2018). Climate change and drought: a perspective on drought indices. *Current climate change reports*, 4:145–163.
- [20] Nam, W.-H., Hayes, M. J., Svoboda, M. D., Tadesse, T., and Wilhite, D. A. (2015). Drought hazard assessment in the context of climate change for south korea. *Agricultural Water Management*, 160:106–117.
- [21] Pillay, R., Venter, M., Aragon-Osejo, J., González-del Pliego, P., Hansen, A. J., Watson, J. E., and Venter, O. (2022). Tropical forests are home to over half of the world's vertebrate species. *Frontiers in Ecology and the Environment*, 20(1):10–15.
- [22] Potapov, P., Li, X., Hernandez-Serna, A., Tyukavina, A., Hansen, M. C., Kommareddy, A., Pickens, A., Turubanova, S., Tang, H., Silva, C. E., et al. (2021). Mapping global forest canopy height through integration of gedi and landsat data. *Remote Sensing of Environment*, 253:112165.
- [23] Saleska, S. R., Didan, K., Huete, A. R., and Da Rocha, H. R. (2007). Amazon forests green-up during 2005 drought. *Science*, 318(5850):612–612.
- [24] Santos, V. A. H. F. d., Ferreira, M. J., Rodrigues, J. V. F. C., Garcia, M. N., Ceron, J. V. B., Nelson, B. W., and Saleska, S. R. (2018). Causes of reduced leaf-level photosynthesis during strong El Niño drought in a Central Amazon forest. *Global Change Biology*, 24(9).

- [25] Souza Jr, C. M., Z. Shimbo, J., Rosa, M. R., Parente, L. L., A. Alencar, A., Rudorff, B. F., Hasenack, H., Matsumoto, M., G. Ferreira, L., Souza-Filho, P. W., et al. (2020). Reconstructing three decades of land use and land cover changes in brazilian biomes with landsat archive and earth engine. *Remote Sensing*, 12(17):2735.
- [26] Tang, H. and Dubayah, R. (2017a). Light-driven growth in Amazon evergreen forests explained by seasonal variations of vertical canopy structure. *Proceedings of the National Academy of Sciences*, 114(10):2640–2644.
- [27] Tang, H. and Dubayah, R. (2017b). Light-driven growth in amazon evergreen forests explained by seasonal variations of vertical canopy structure. *Proceedings of the National Academy of Sciences*, 114(10):2640–2644.
- [28] Tang, H., Dubayah, R., Swatantran, A., Hofton, M., Sheldon, S., Clark, D. B., and Blair, B. (2012). Retrieval of vertical lai profiles over tropical rain forests using waveform lidar at la selva, costa rica. *Remote Sensing of Environment*, 124:242–250.
- [29] Vicente-Serrano, S. M., Beguería, S., and López-Moreno, J. I. (2010). A multiscalar drought index sensitive to global warming: the standardized precipitation evapotranspiration index. *Journal of climate*, 23(7):1696–1718.
- [30] Walker, L. R., Wardle, D. A., Bardgett, R. D., and Clarkson, B. D. (2010). The use of chronosequences in studies of ecological succession and soil development. *Journal of ecology*, 98(4):725–736.
- [31] Wells, N., Goddard, S., and Hayes, M. J. (2004). A self-calibrating palmer drought severity index. *Journal of climate*, 17(12):2335–2351.
- [32] Yihdego, Y., Vaheddoost, B., and Al-Weshah, R. A. (2019). Drought indices and indicators revisited. *Arabian Journal of Geosciences*, 12:1–12.

Appendix A

Supplementary materials

A.1 Definitions

A.1.1 Dry seasons, dry months, dry forests

The definitions in this section were extracted from the existing literature and used as reference. Dry month is a month which receives less than 100mm of total precipitation. We calculated average dry season periods across 22 years of climatic data. Dry seasons are periods with dry months or consecutive months that cumulatively receive less than one third of the annual precipitation amount. Regions where monthly minimum precipitation exceeds 150mm are classified as regions without dry seasons [26].

We can classify regions 6, 7 and 8 as seasonally dry tropical forests, using the definition of mean annual temperature above 17°C, between 200-2500 mm annual rainfall, and an annual ratio of potential evapotranspiration to precipitation greater than 1 [1].

A.2 Seasonality

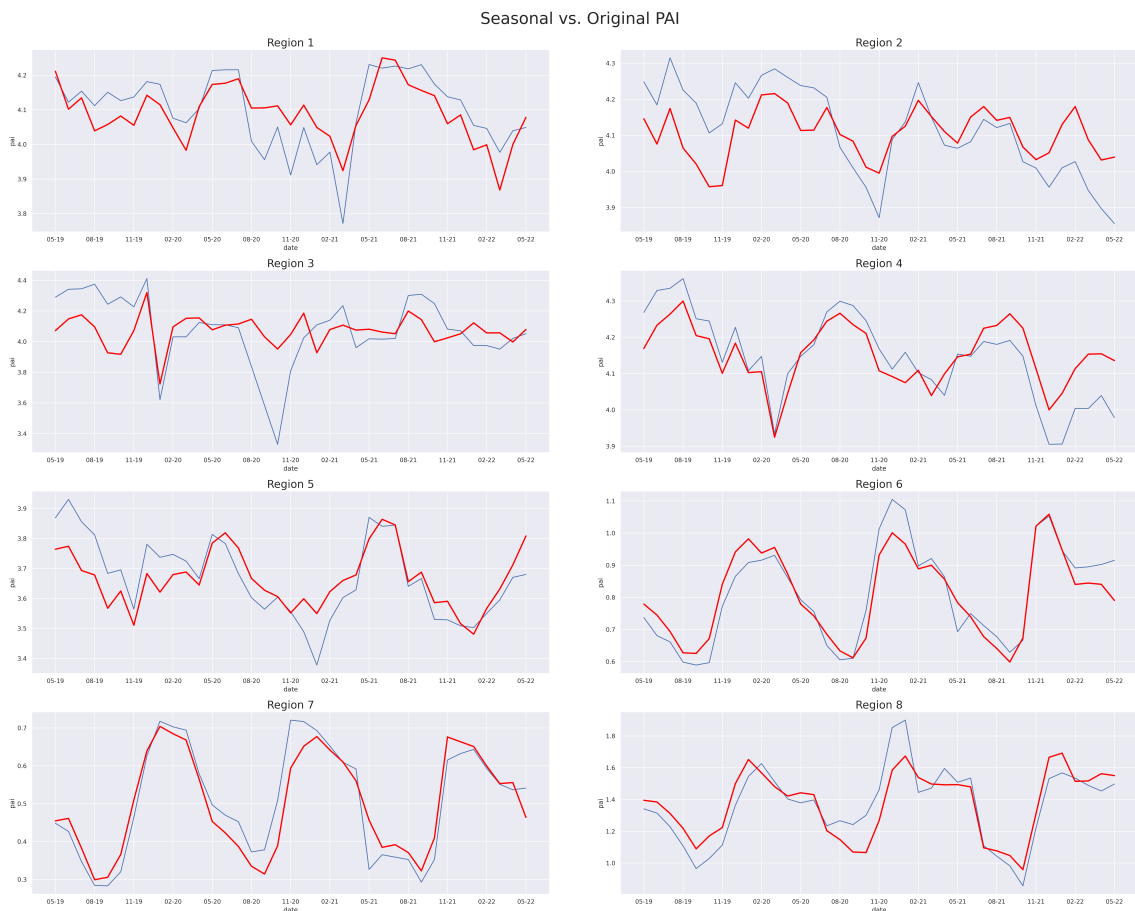


Fig. A.1 – Seasonal component of PAI vs. original data.

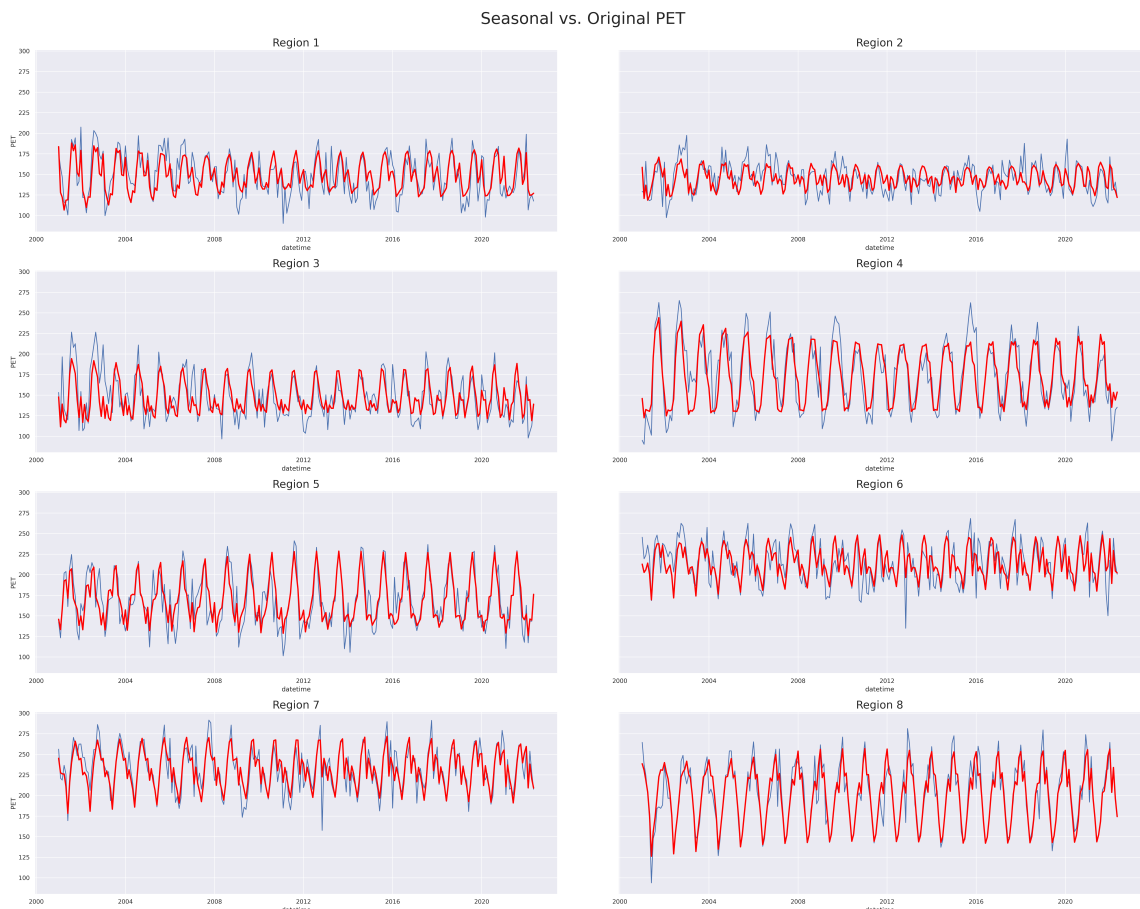


Fig. A.2 – Seasonal component of PET vs. original data.

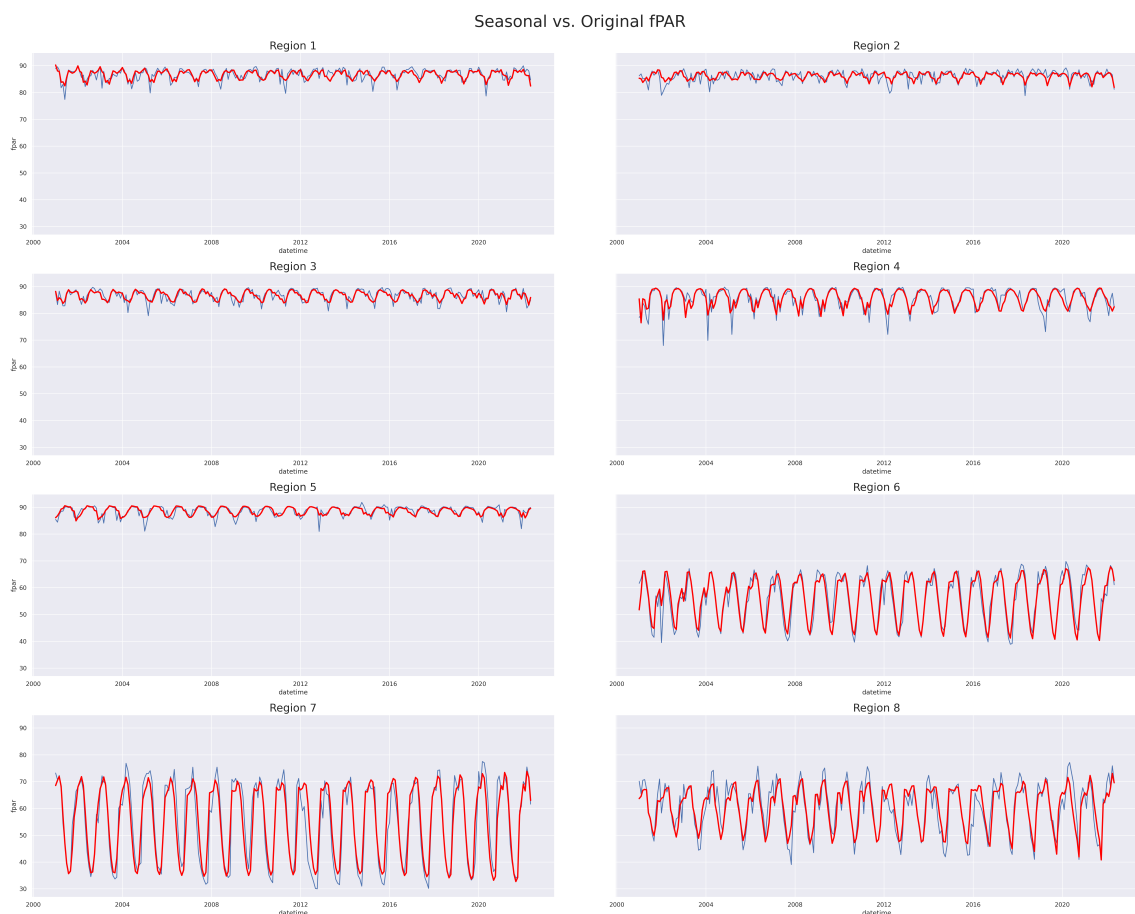


Fig. A.3 – Seasonal component of FPAR vs. original data.

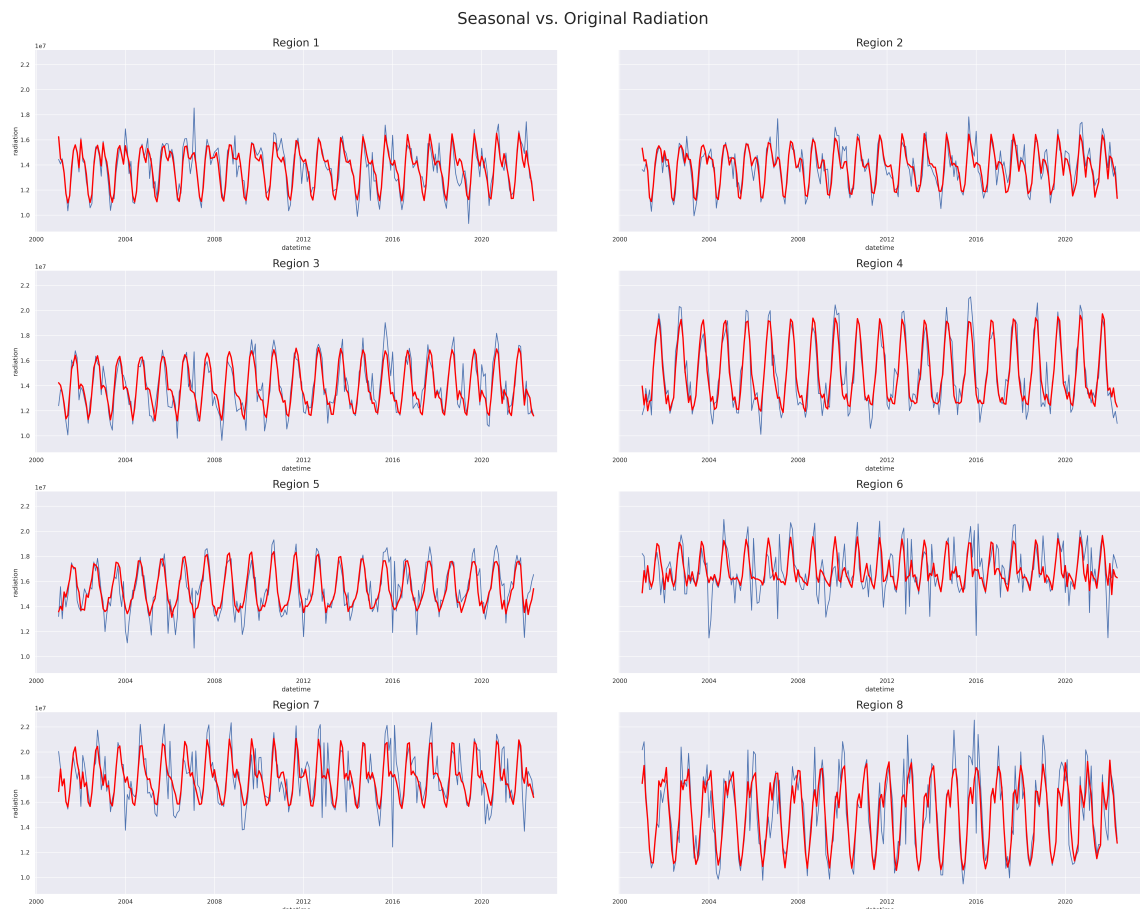


Fig. A.4 – Seasonal component of radiation vs. original data.

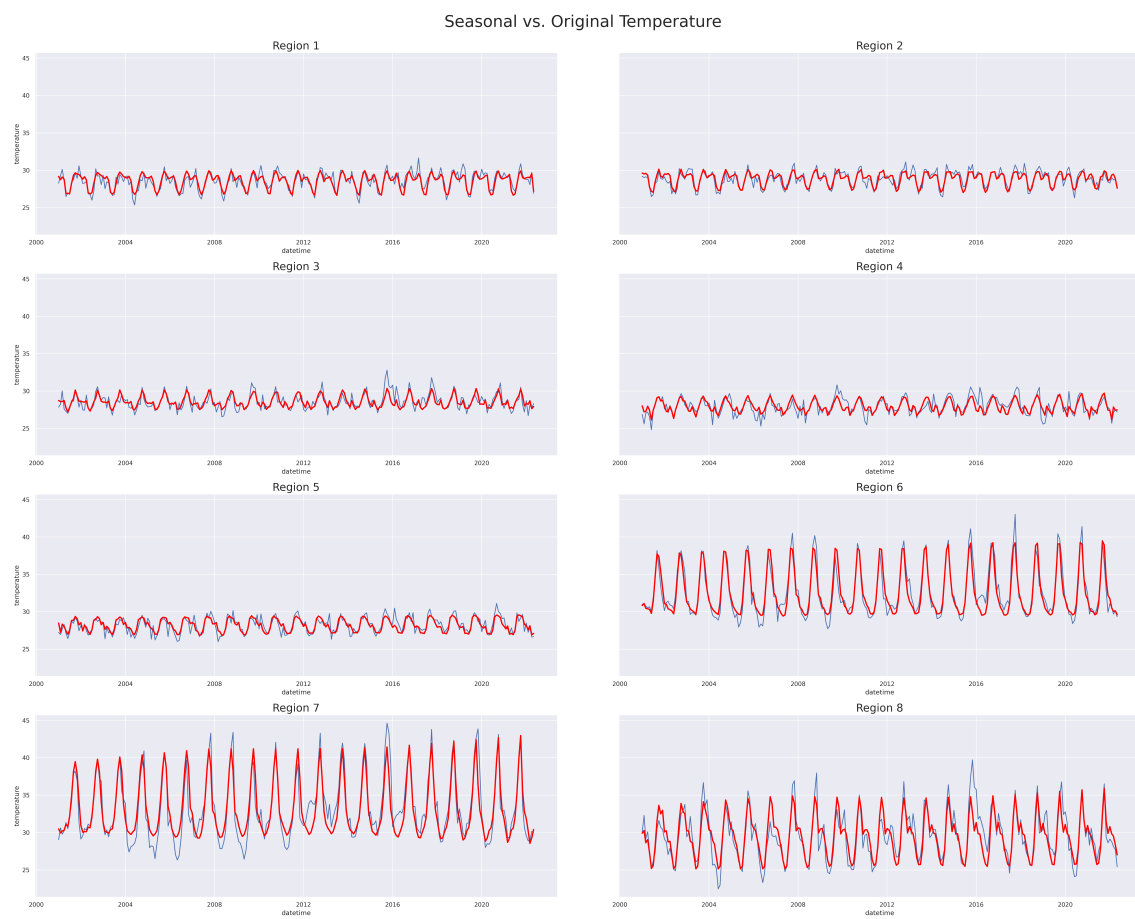


Fig. A.5 – Seasonal component of temperature vs. original data.

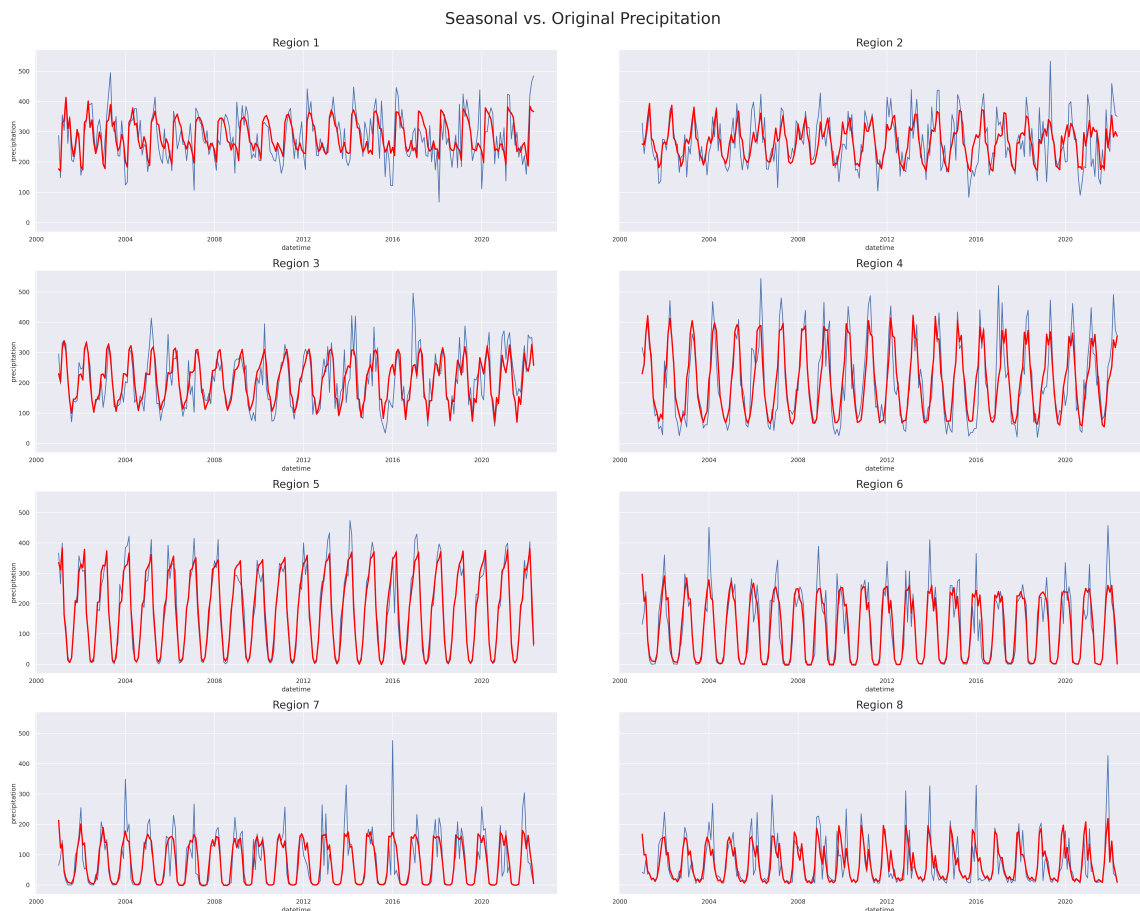


Fig. A.6 – Seasonal component of precipitation vs. original data.

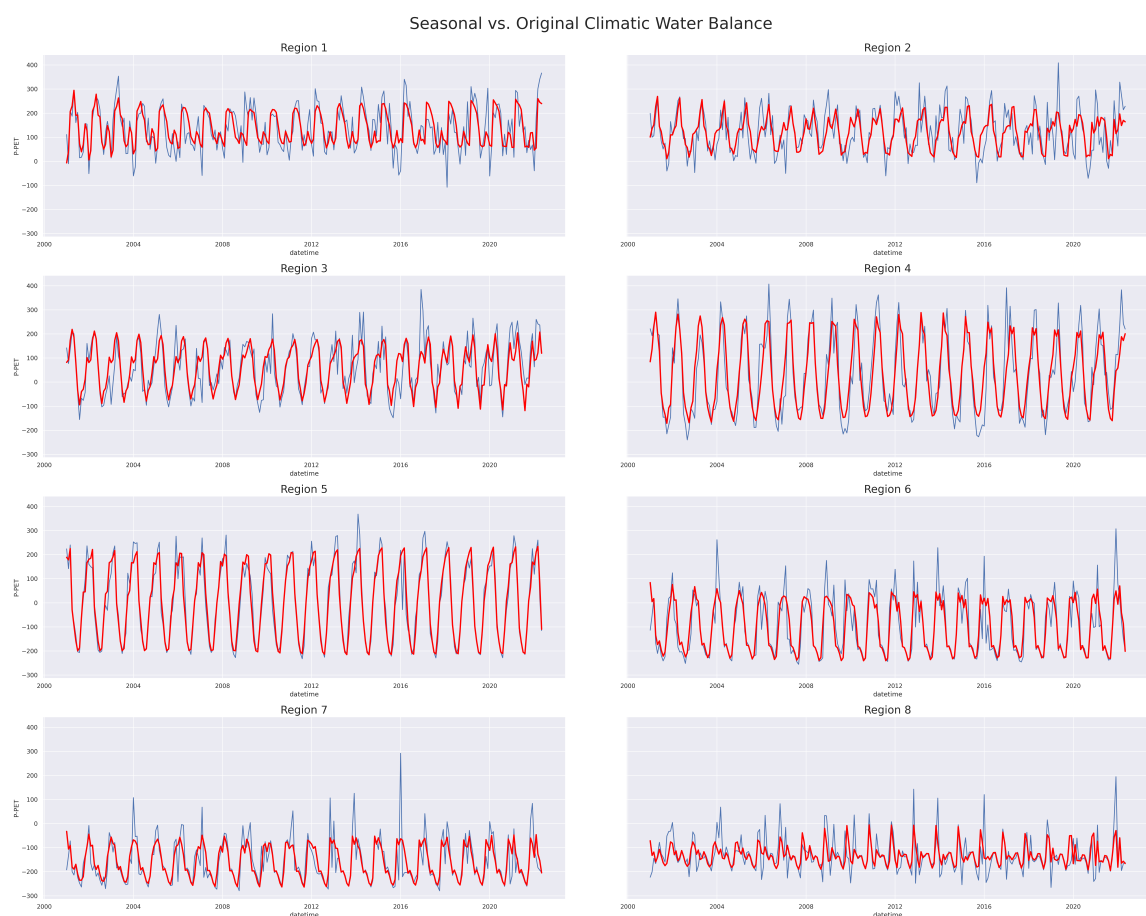


Fig. A.7 – Seasonal component of climatic water balance vs. original data.

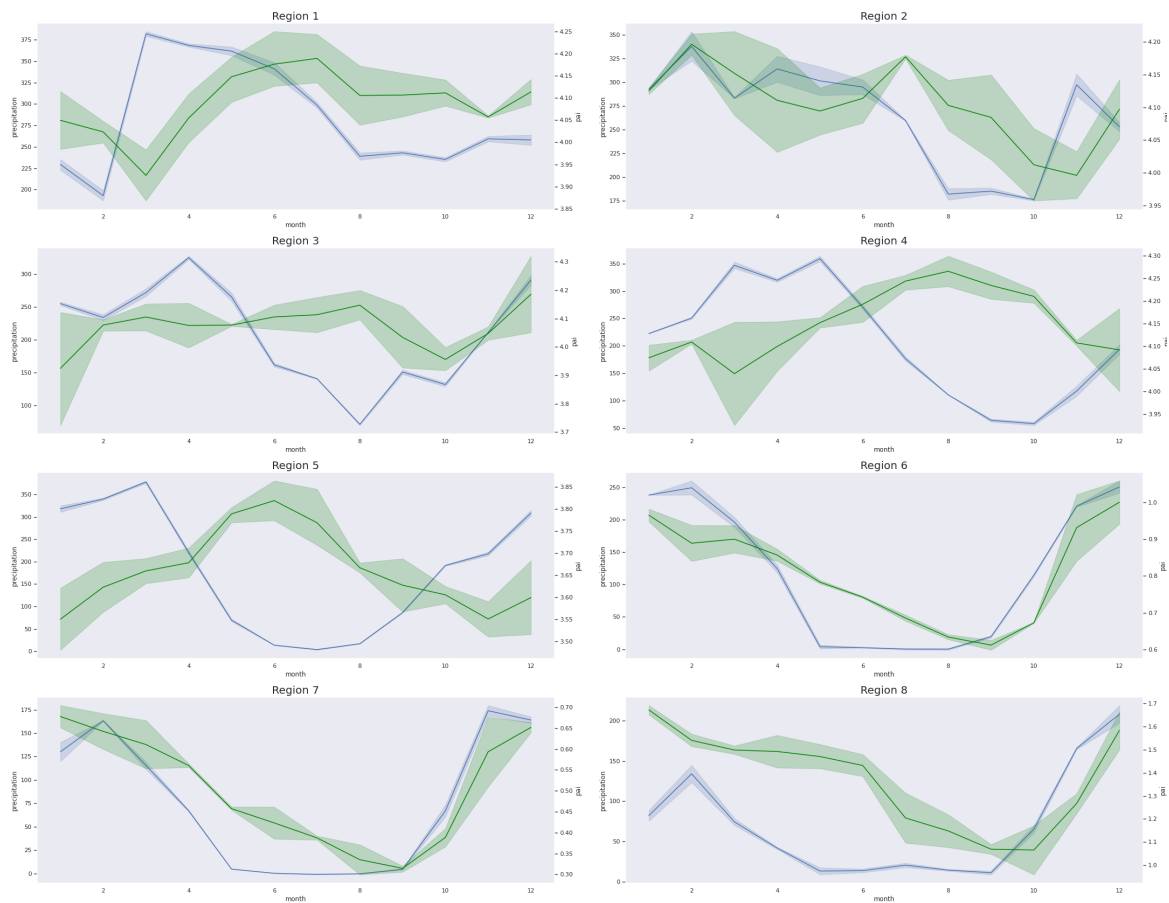


Fig. A.8 – Comparison of the seasonality between PAI and precipitation. For each variable, we aggregate the seasonal components across years to generate a yearly average of the monthly seasonality.

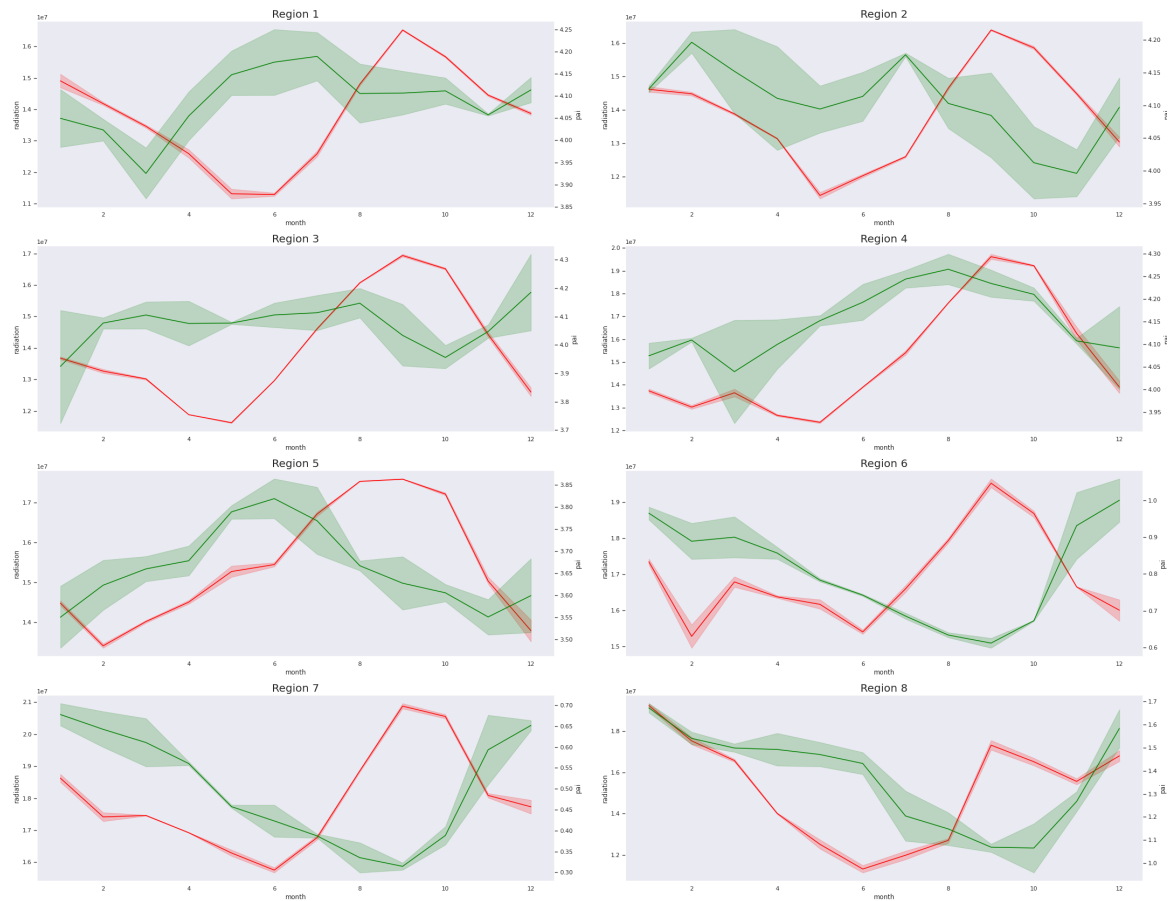


Fig. A.9 – Comparison of the seasonality between PAI and precipitation. For each variable, we aggregate the seasonal components across years to generate a yearly average of the monthly seasonality.

Table A.1 – Correlation coefficients between the seasonal PAI and climate variables

Region	1	2	3	4	5	6	7	8
precipitation ₋₂	-0.544	-0.035	-0.347	-0.821	-0.788	0.151	0.034	-0.449
precipitation ₋₁	-0.347	0.037	-0.057	-0.739	-0.791	0.551	0.490	-0.093
precipitation ₀	-0.018	0.368	0.011	-0.507	-0.613	0.837	0.860	0.373
precipitation ₁	0.537	0.556	0.005	-0.086	-0.261	0.865	0.917	0.770
precipitation ₂	0.598	0.500	0.159	0.338	0.249	0.613	0.699	0.756
radiation ₋₂	0.548	-0.080	0.233	0.741	0.779	-0.508	-0.572	-0.326
radiation ₋₁	0.137	-0.021	0.101	0.803	0.568	-0.624	-0.507	0.022
radiation ₀	-0.250	-0.243	-0.202	0.580	0.165	-0.546	-0.281	0.223
radiation ₁	-0.410	-0.454	-0.178	0.226	-0.185	-0.170	0.152	0.429
radiation ₂	-0.446	-0.476	-0.177	-0.194	-0.468	0.428	0.626	0.710
temperature ₋₂	0.100	-0.091	0.067	0.727	0.320	-0.740	-0.814	-0.584
temperature ₋₁	-0.445	-0.036	-0.132	0.710	-0.174	-0.736	-0.798	-0.510
temperature ₀	-0.560	-0.277	-0.290	0.423	-0.596	-0.479	-0.503	-0.304
temperature ₁	-0.455	-0.386	-0.092	0.149	-0.743	0.053	0.037	0.154
temperature ₂	-0.224	-0.209	-0.108	-0.221	-0.664	0.615	0.523	0.702
fpar ₋₂	0.596	-0.311	0.210	0.742	0.668	0.669	0.717	0.483
fpar ₋₁	0.158	0.083	0.085	0.792	0.737	0.820	0.900	0.722
fpar ₀	-0.289	0.116	-0.112	0.592	0.531	0.767	0.845	0.843
fpar ₁	-0.428	-0.180	-0.050	0.247	0.293	0.467	0.499	0.639
fpar ₂	-0.606	-0.410	-0.328	-0.183	-0.190	-0.049	0.041	0.099
P-PET ₋₂	-0.588	0.012	-0.326	-0.801	-0.815	0.200	0.199	-0.346
P-PET ₋₁	-0.412	-0.002	-0.117	-0.778	-0.793	0.593	0.596	-0.125
P-PET ₀	-0.069	0.278	0.003	-0.576	-0.576	0.872	0.892	0.216
P-PET ₁	0.458	0.516	0.018	-0.178	-0.203	0.856	0.823	0.548
P-PET ₂	0.588	0.545	0.165	0.255	0.278	0.517	0.492	0.442